Competition between photoexcitation and relaxation in spin-crossover complexes in the frame of a mechanoelastic model

Cristian Enachescu,[1,*] Laurentiu Stoleriu,[1] Alexandru Stancu,[1] and Andreas Hauser[2]
[1]*Department of Physics, Alexandru Ioan Cuza University, Iasi, Romania, EU*
[2]*Département de Chimie Physique, Université de Genève, Geneva, Switzerland*
(Received 19 May 2010; revised manuscript received 14 August 2010; published 21 September 2010)

In this paper we use a recently proposed elastic model in order to study the competition between linear photoexcitation and cooperative relaxation in spin-crossover molecular magnets. The difference in molecular size between the two possible spin states, that is, the high-spin and the low-spin states, respectively, induces distortions of the crystal lattice. These determine the elastic interactions between molecules, treated here as connecting springs that are either compressed or extended from their equilibrium length, thus modulating the local probability for the high-spin→low-spin relaxation. The crossover of individual molecules within the lattice is checked by a standard Monte Carlo procedure. Using very simple assumptions and a minimum number of parameters, photoexcitation curves and hysteresis loops under continuous irradiation below the thermal transition temperature can thus be simulated. The formation of clusters is analyzed and the presence of inhomogeneities in the system is investigated.

DOI: 10.1103/PhysRevB.82.104114 PACS number(s): 64.60.−i, 75.30.Wx, 75.60.−d

I. INTRODUCTION

The exponential advances of magnetic recording technologies, which we have witnessed over the last three decades, have produced 1 TB memories[1] and opened the perspective of a further increase by an order of magnitude within the next decade. However, the bit-patterned media, which are the best magnetic candidates for such recording densities, have exposed a number of technological problems and limitations that are now intensely studied. Nevertheless, genuine physical limits for the studied solutions seem to be unavoidable, and consequently new materials and fresh ideas have to be considered and need to be investigated.

Spin-crossover solids are a potential solution for the recording media of the future, as they can be switched by a range of physical perturbations such as variable temperature, applied pressure, or electromagnetic radiation. In the last few years, their study produced an avalanche of remarkable results including synthesis of spin crossover neat nanoparticles[2] or of nanoparticles covered with a surfactant[3] or chitosan,[4] the production of nanoscale films of a spin-crossover polymer growing on a gold surface,[5,6] and the switching at room temperature in both directions within the hysteresis loop.[7,8]

Spin-crossover solids are molecular compounds belonging to the class of molecular magnets and they are switchable between two states in thermodynamic competition: the diamagnetic low-spin (LS) state and the paramagnetic high-spin (HS) state, with different magnetic and optical properties, unit-cell volumes and metal-ligand bond lengths. Both unit-cell volume and bond length are considerably larger for the HS state, resulting, in addition to the larger electronic degeneracy, also in a larger phonon density for this state. Thus, due to thermodynamic considerations, the LS state is the stable state at low temperatures, but it can be transformed to the metastable HS state by irradiation with an appropriate wavelength—the so-called light-induced excited spin-state trapping (LIESST) effect.[9,10] If the light is switched off, the HS state relaxes back to the stable LS state by the way of a nonradiative process. The competition between relaxation and photoexcitation in the case of cooperative (highly interacting) systems can result in light-induced hysteresis behavior[11] or light-induced thermal hysteresis (LITH) and light-induced optical hysteresis under continuous irradiation.[12] The evolution of the system is usually described by the fraction of molecules in the HS state, denoted here as n_{HS}.

Basically, the different volumes of the molecules in the two spin states are at the origin of the elastic stresses in the crystalline network. These determine the cooperative effects and thus the variation in the switching probability with the HS fraction. This elastic interaction between the molecules is usually modeled as a superposition of two components: a short-range interaction, statistically distributed within the sample, and a long-range interaction proportional to the average number of HS molecules per unit volume. While the mean-field models cannot explain the behavior of spin-crossover compounds with specific nearest-neighbor interactions,[13,14] Ising-type models considering both short- and long-range interactions have satisfactorily reproduced several of the more unusual features of cooperative behavior.[13,15–17] In the models based on the ball and spring concept, the effective interactions not only depend on the states of interacting molecules and on the HS fraction, but they are directly influenced by the local elastic distortions resulting from the molecular volume change during the transition. A first approximation implied the separation of distortions in each one-dimensional direction.[18,19] Recent models have been developed in two-dimensional (2D) or three-dimensional (3D) rectangular systems with periodical boundary conditions, using molecular-dynamics[20] or standard Monte Carlo Metropolis methods,[21] but also in finite bidimensional hexagonal lattices.[22,23]

The study of light-induced effects in spin-crossover solids has become increasingly relevant over the last few years because of their possible use as fully optical memory devices.[24] Experimental research has been conducted to determine the quantum efficiency of the photoexcitation[25] or to investigate

the switching time itself[26] while models have been developed to study various hysteresis types under light[14] or threshold phenomena under photoexcitation.[27] In this paper we use the simple but realistic mechanoelastic model[23] to explain the wide range of complex processes under irradiation in spin-crossover compounds, including nonlinear photoexcitation curves, bistability, hysteresis, and the behavior of nonhomogenous systems. We begin by presenting the key elements of the model, in which a single spring constant describes both of the above-mentioned interaction types. We then proceed to a discussion of the results of the model, followed by a comparison with experiment and similar approaches in the literature.

II. MODEL

In the mechanoelastic model[23] the spin-crossover units (molecules) are represented as rigid spheres connected by springs and are situated in a 2D hexagonal lattice.[22,23] Besides the fact that there are several spin-crossover complexes showing hexagonal structures such as $[Fe(bbtr)_2](ClO_4)_2$ (Refs. 28 and 29) and $[Fe(dpa)(NCS)_2]_2bpym$,[30] the hexagonal structure requires only one single spring constant and is more stable than 2D rectangular lattices. For the latter, an additional diagonal spring constant between the molecules situated at the opposite corners had to be introduced in order to ensure geometrical stability of the system.[20,21,27,31,32] Consequently, the use of a hexagonal lattice keeps the number of parameters needed to describe the system at a minimum.

Initially, all the molecules are considered to be in the same state (either the LS or the HS state). In these limiting situations and as long as no external forces act on them as a result of an external pressure, all springs are considered unstressed. In a mixed system with a given HS fraction, the individual springs are no longer unstressed. Depending upon the state of a molecule and the states of its neighbors, springs may be either compressed or extended and thus exert a nonzero force or local pressure on this molecule. In a second stage, we can apply an external pressure simulated by forces acting on edge molecules and oriented in the direction of missing springs (Fig. 1). All the springs are then compressed and the same local forces from this pressure act on all molecules.

At any time, the probability for a given molecule to switch from the HS to the LS state, $P^i_{HS\to LS}$, depends on the temperature and on the forces acting on the molecule from its neighbors, while under the assumption that the intersystem crossing probabilities of LIESST do not depend upon the HS fraction, the probability for a molecule to switch from the LS to the HS state, $P^i_{LS\to HS}$, is constant and is related to the intensity of irradiation as in the low-temperature region the probability for a thermal LS to HS transition is negligible,

$$P^i_{HS\to LS} = k_0 \exp\left(-\frac{E_a - \kappa p_i}{k_B T}\right),$$

$$P^i_{LS\to HS} = \omega, \tag{1}$$

where k_0 is a scaling factor, E_a is the activation energy in the absence of interactions, which is therefore the same for all

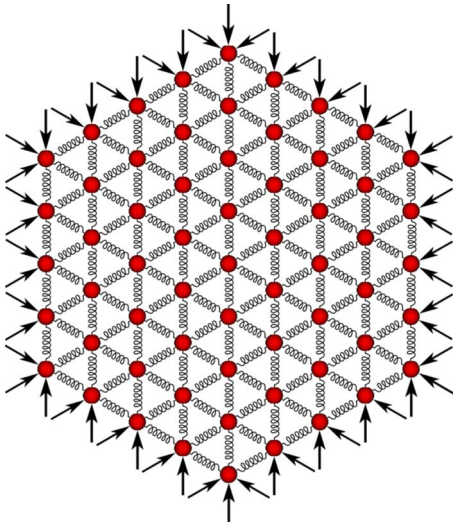

FIG. 1. (Color online) Model of the 2D hexagonal lattice considered in the simulation and the way that external pressure acts on edge and corner particles.

molecules, T is the temperature, p_i the local pressure acting on the ith molecule, κ a scaling constant that establishes to which extent the local pressure influences the relaxation probability, k_B the Boltzmann constant set here equal to unity while ω is a term proportional to the irradiation intensity and the absorption cross section at the irradiation wavelength.

The local pressure for a given molecule is calculated in a local mean-field approximation as the sum of forces per unit area applied to that molecule by all neighboring springs (six for inside molecules, four for edge molecules, and three for corner molecules),

$$p_i = \sum_{nearest\ \ neighbors} k\delta x_i + p, \tag{2}$$

where k is the spring constant divided by unit area and p is the external pressure that replaces every missing spring in the case of edge molecules and is perpendicular to the lattice. As we have stated above, the local pressure can be different for every molecule, influencing the HS to LS switching probability (see Fig. 2). Neither state is favored if the local pressure is zero [Figs. 2(a) and 2(b)]. If the springs near a HS molecule are elongated [Fig. 2(c)], then they will act toward increasing the molecular volume, so the probability that this molecule passes to the smaller volume LS state is lower. This corresponds to a negative local pressure in the probability $P^i_{HS\to LS}$. Reversely, if the springs near a HS molecule are compressed, the probability that the molecule passes to the LS state is higher [positive local pressure, Fig. 2(d)].

The temporal evolution of the system is simulated following a standard Monte Carlo algorithm. (i) In a sequential process, we check every molecule in the system to verify whether it switches or not by first calculating its state-dependent switching probability and then generating a random number $\eta \in (0,1)$. If this number is smaller than the probability then the molecule is allowed to change its state, otherwise it stays in the same state. A Monte Carlo step is concluded when all molecules in the system have been

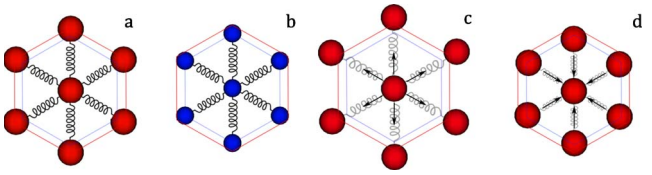

FIG. 2. (Color online) Possible situations for a central molecule and its nearest neighbors: (a) all molecules in the HS state and no local pressure acting on the central molecule, (b) all molecules in the LS state and no local pressure acting on the central molecule, (c) a negative local pressure acting on the central HS molecule, and (d) a positive local pressure acting on the HS central molecule. In all presented situations the mechanical equilibrium condition is respected. The external red full lines hexagon corresponds to the equilibrium positions when all molecules are HS while the dotted blue hexagon corresponds to the equilibrium position when all molecules are LS.

checked once. (ii) As a state change in a molecule results in a volume change in the molecular sphere around 10% instantaneous forces will appear inside neighboring springs that will determine at first the shift in position of neighbor molecules and then progressively of all other molecules in the system. The molecules stop moving when all of them are in mechanical equilibrium, i.e., the resulting force on every molecule is zero ($\Sigma_{neighbour\ springs} k\delta\vec{x}_i + \vec{p} = 0$, where $\vec{p}$ is the pressure force taken into account only for edge molecules).

In order to find the equilibrium positions for all molecules in the system after every Monte Carlo step, we consider that each molecule has a damped oscillatory-type motion. The equilibrium nuclear configuration is then found by iteratively solving the following system of $2 \times n$ coupled differential equations (n being the number of molecules),

$$\begin{cases} m\dfrac{d^2x_i}{dt^2} = F_{xi} - \mu\dfrac{dx_i}{dt} \\ m\dfrac{d^2y_i}{dt^2} = F_{yi} - \mu\dfrac{dy_i}{dt}, \end{cases} \tag{3}$$

until the equilibrium is established as mentioned previously. The following notations have been used: x_i, y_i are the Cartesian coordinates of molecule i, μ is the damping constant, and F_{xi}, F_{yi} are the algebraic sums of forces acting on particle i in the two directions. The system of equations is solved using the DIVPAG routine for stiff ordinal differential equations from the IMSL Math Library based on the Gear's BDF (Backward Differentiation Formulas) method.[33] A short discussion about the effect of the damping parameter on the equilibrium is presented in Appendix.

In the simulations presented below, the size of the system has been chosen large enough (from 2791 to 30 313 molecules) in order to minimize the size and edge effects typical for open boundary systems.[23]

III. RESULTS AND DISCUSSIONS

Photoexcitation curves calculated in the framework of the present model for different light intensities are presented in Fig. 3. The photoexcitation curves are close to single exponential if the irradiation intensity is high such that the excitation rate is higher than the relaxation rate. The photoexcitation time in this case is directly proportional to the intensity and the final metastable HS fraction obtained is close to saturation. If the light intensity decreases, then the role played by relaxation becomes significant: the sample cannot be saturated anymore and a steady state is established at lower values of the HS fraction. For even lower intensities, the photoexcitation curve changes into a sigmoidal shape. This shape is obtained here not because of some possible cooperative effects intrinsic to the photoexcitation or to some variations in the quantum efficiency with the HS fraction,[25,34] but it can be simply understood only on the basis of the self-accelerated character of the cooperative HS→LS relaxation.[25,35,36] As in the classical mean-field approach, the effect of the relaxation is most prominent at low values of the HS fraction, where the actual relaxation rate constant is largest. If the irradiation intensity is lower than a threshold value, then the excitation is not sufficiently fast to overcome the relaxation, so the photoexcitation levels off at a steady-state value of the HS fraction close to zero. As the steady state is not an equilibrium state, there are fluctuations of and the configuration of the system changes at every Monte Carlo step.

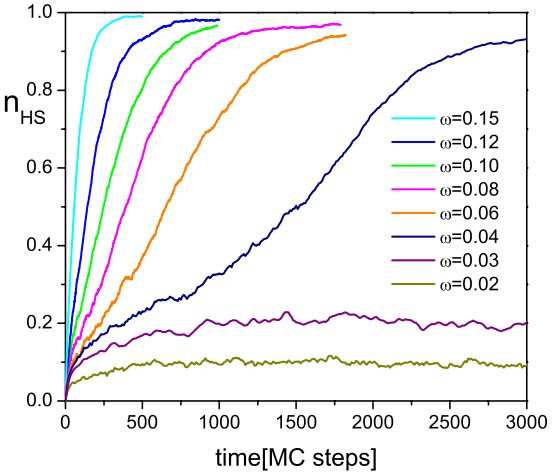

FIG. 3. (Color online) Photoexcitation curves in the presence of relaxation for various values of the irradiation intensity ω. The sigmoidal shape of the photoexcitation curve for lower values of the intensity (ω=0.04) is the effect of the competition between relaxation and photoexcitation. The other parameters are: E_a=400 K, T=50 K, κ=1000, p=0.01, k=1 N/m, and μ=1 N s/m.

In a recent paper, we showed that during the HS→LS relaxation process, clusters form starting from the edges of the system, whereas during the thermal transition clusters grow from corners for both the present model[37] as well as molecular-dynamics models.[38] The existence of HS and LS domain nucleation processes has been confirmed experimentally by x-ray diffraction[39,40] and by optical microscopy.[41,42] In Fig. 4 we present snapshots of the system for three different values of the irradiation intensity each taken at a HS fraction equal to 0.2 on the respective excitation curve. If the photoexcitation intensity is high enough (Fig. 4, left), then no clusters are formed and the molecules switch from the LS to the HS state independently of each other, as the random

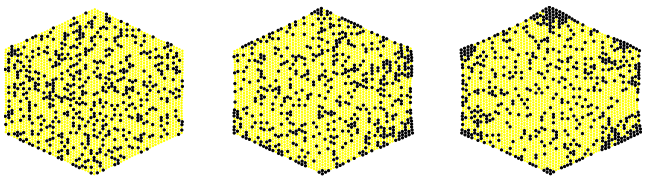

FIG. 4. (Color online) Snapshots at a HS fraction of 0.2 during photoexcitation at different irradiation intensities: at high intensity (left, ω=0.2) no cluster are formed; at medium intensity just high enough to overcome the relaxation (middle, ω=0.04) the photoexcitation starts from corners and edges; and low intensity that creates a steady state under continuous irradiation (right, ω=0.02) cluster form mainly at corners. Yellow circles correspond to LS sites and black circles to HS sites.

character of the light-induced process tends to destroy the correlations inside the sample, which otherwise spontaneously buildup during relaxation.[16] This situation corresponds to the mean-field behavior. In the case of a lower intensity (Fig. 4, middle), when the competition between photoexcitation and relaxation is effective, deviations from the mean-field behavior are observed and the buildup of correlations results in nonrandom distributions of HS and LS molecules. Consequently, HS clusters created by nucleation and growth phenomena can be detected starting from borders. Finally if the intensity is so low that it can no longer overcome the relaxation (Fig. 4, right), a steady state under continuous irradiation establishes itself and HS clusters occupy the corners. This situation is different compared to the HS→LS relaxation in the dark, for which clusters preferentially form from edges and not necessarily from corners.[23]

It is interesting to compare our results obtained for an open boundary lattice of spring-connected molecules with those for a periodic system with analogous interactions induced by local elastic distortions.[27] In both systems, threshold phenomena occur and the change in the shape of photoexcitation curves with irradiation intensity is similar. However, in the periodic systems no visible clusters are observed even for highly interacting molecules.[27]

For some intermediate values of light intensity and at a temperature where the relaxation is in competition with the excitation, a bistability under continuous irradiation can be observed, which is a direct consequence of the cooperative relaxation that determines also the sigmoidal photoexcitation curves. Depending on the initial configuration of the system, one or the other of the two steady states is obtained: the lower one if at the starting point the system is purely in the LS state and the higher one if we start from the pure HS state. If the initial state of the system is in between the two steady states, then the system relaxes toward one of these states, depending on whether the departure point is below or above the bifurcation point. Figure 5 shows that for a small system (2791 molecules) the comparatively large fluctuations direct the system quite quickly toward one of its steady states. For larger systems (30 313 molecules) the relaxation time becomes longer as shown in the inset of Fig. 5. This dependence is similar to that observed for the bidimensional system treated by Miyashita *et al.*[27] using molecular dynamics. These authors showed that the lifetime of metastable

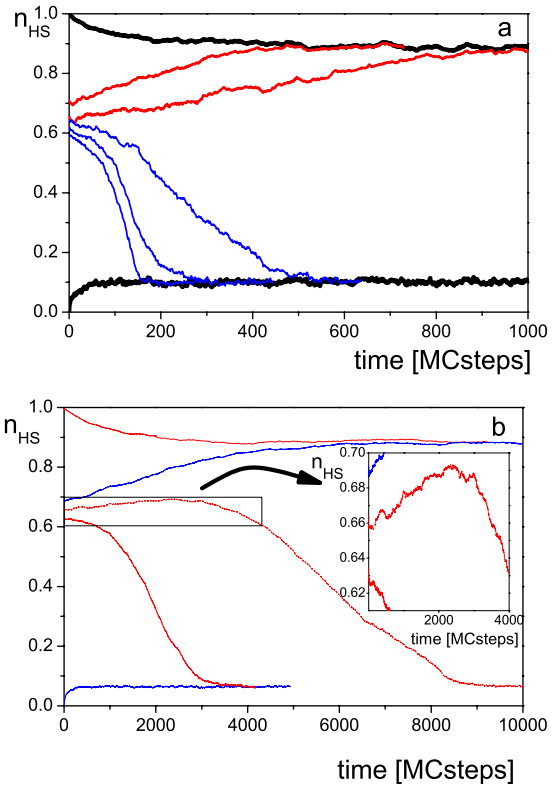

FIG. 5. (Color online) Bistability at low temperature: depending on the starting point, one of the two steady states can be obtained. Curves were obtained for a system (a) of 2791 molecule and (b) of 30 313 molecules. The inset of panel (b) shows the initial stage of the evolution at an enlarged scale. The broken line starting from a random distribution near the bifurcation point starts with an increasing HS fraction but nevertheless converges to the lower branch of the steady-state HS fraction. The photoexcitation rate is ω=0.02 and all the others parameters are those given in the caption of Fig. 3.

states increases exponentially with the size of the system and contrasts with the case of short-range interaction models, in which local nucleation takes place.[43] The so-called phase separation phenomenon associated with inhomogeneities inside samples can be identified by the presence of some erratic bumps in the asymptotic branches of the curves under photoexcitation. Such inhomogeneities were previously observed experimentally[12,34] and can occur spontaneously, either due to the thermal fluctuations or resulting from an inhomogeneous thermal or optical treatment of the sample.

A seemingly paradoxical evolution of the HS fraction is put in evidence in the inset of Fig. 5(b): after starting from a point with a random configuration and situated near the bifurcation point, it initially increases, until the system finds an appropriate internal order and then decreases until it reaches the lower branch of the steady-state HS fraction. Indeed, this evolution is in line with several hitherto difficult to understand experimental effects under continuous irradiation observed previously by Varret *et al.*[14]

A direct consequence of the light-induced bistability is the presence of several types of hysteresis behavior under continuous irradiation, the most important of which is the LITH.[12,14,44] At low temperatures the relaxation is slow so

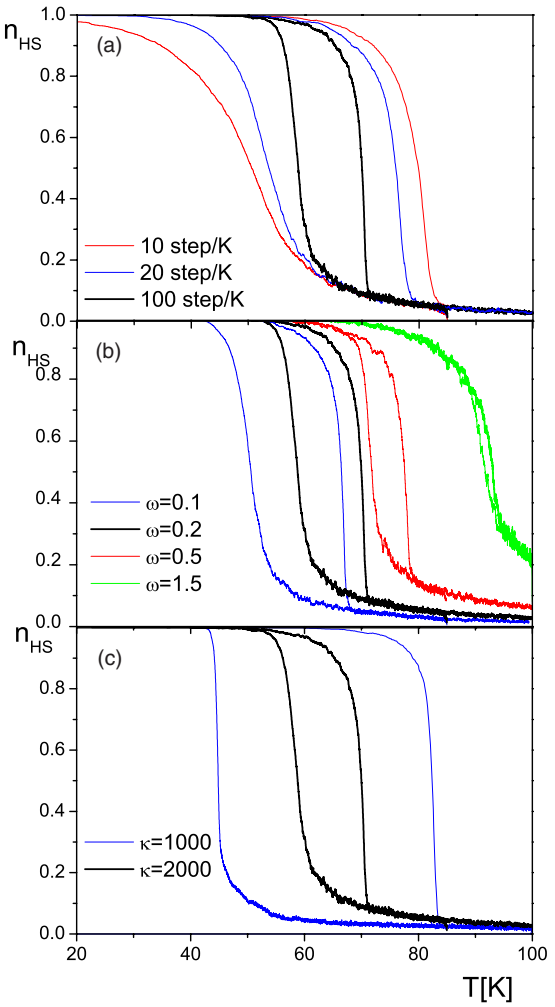

FIG. 6. (Color online) Light-induced thermal hysteresis: (a) dependence on temperature sweep rate, (b) irradiation intensity, and (c) interaction strength. The other system parameters are those specified in Fig. 3.

the photoexcitation dominates and the complexes are essentially in the HS state while due to the fast relaxation at higher temperatures complexes will be the LS state. In between, there is a temperature range in which the two processes compete. If the interactions are weak, only a single photostationary state is established at all times, with a continuously lower steady state HS fraction for increasing temperatures. Above a threshold value of the interactions, two steady states can be obtained as described above. The corresponding hysteresis loop moves to higher temperature with increasing irradiation intensity and its width increases with stronger interactions. As both the relaxation and the photoexcitation are intrinsically kinetic phenomena, the LITH loops are very sensitive to the temperature sweep rate.

The dependence of the LITH curves on the various parameters can be reproduced within the framework of the present model and are summarized in Fig. 6. Of particular and practical importance for the experimentalist is the temperature sweep rate. As demonstrated by Fig. 6(a), very small and often prohibitively small values of the temperature sweep rates have to be chosen in order to approach the

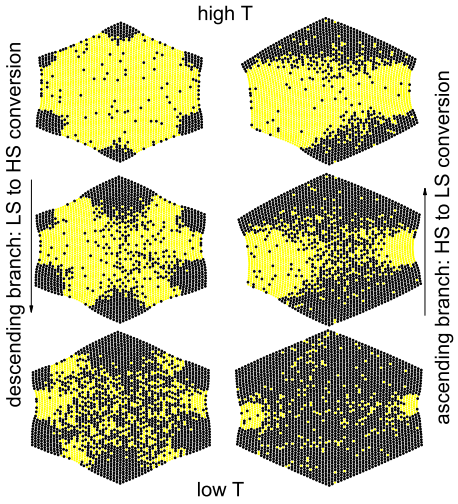

FIG. 7. (Color online) Evolution of the system from LS to HS on the descending branch of the LITH at n_{HS}=0.15, 0.35, and 0.6 (on the left top to bottom): HS clusters start from corners. Evolution of the system from HS to LS on the ascending branch of the LITH at n_{HS}=0.85, 0.7, and 0.4 (on the right top to bottom): LS clusters start from edges, not necessary from corners. Yellow circles correspond to LS sites and black circles to HS sites

steady-state LITH. Even moderate temperature sweep rates quickly result in a kinetic broadening of the LITH. This can be somewhat remedied by using higher irradiation intensities, which shift the LITH toward higher temperatures where the relaxation processes are faster. However, the shift is bigger for the lower temperature branch, and consequently the width of LITH decreases with increasing irradiation intensity, at the critical value the LITH is expected to disappear. This is shown in Fig. 6(b). Finally the dependence of the width of the LITH on the interaction strength is demonstrated in Fig. 6(c).

Figure 7 shows the evolution of the HS and LS molecules along both branches of the black reference LITH of Fig. 6. For both branches, clustering is observed. For the descending branch (Fig. 7, left panel) HS clusters start to form from corners, as is also the case for low-temperature irradiation, whereas for the ascending branch, the LS clusters start from edges, similar to the HS→LS relaxation in the dark at low temperatures. It was pointed out that the clusters could start from the corners even for the ascending branch if considering the LS to HS relaxation, together with a very high irradiation intensity, that would bring the LITH close to the thermal transition.[45]

An important challenge for experimental relaxation curves in strongly cooperative systems is to obtain a fully saturated state at the beginning of the experiment, that is, when the light is switched off. Incomplete photoexcitation, unless carefully engineered on purpose by the proper choice of irradiation conditions,[16] can produce inhomogeneities in the distribution of the light-induced HS state. These distributions are responsible for a faster start of the relaxation, which smears out the characteristic sigmoidal shape of the relaxation curves in strongly cooperative systems. In extremis, they result in a shape of a stretched exponential,[34] thus hiding the characteristics of the cooperative relaxation. Even a

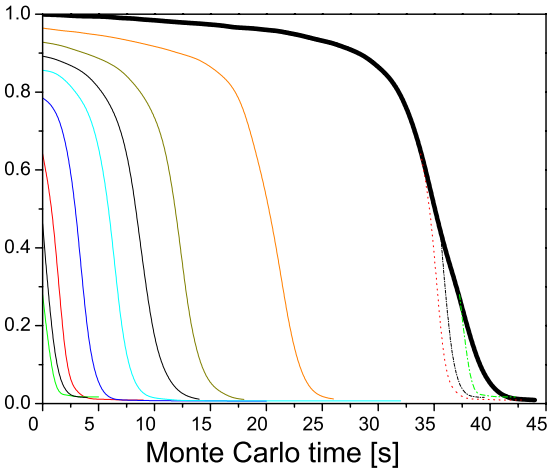

FIG. 8. (Color online) HS→LS relaxation curves for complete excitation (thick line) and from incomplete photoexcitation with an initial random distribution: the sigmoidal shape slowly becomes less pronounced as the initial HS fraction decreases. For direct comparison the curves for partial relaxation are also shown shifted so that the initial value coincides with the value of the full relaxation curve (dotted lines).

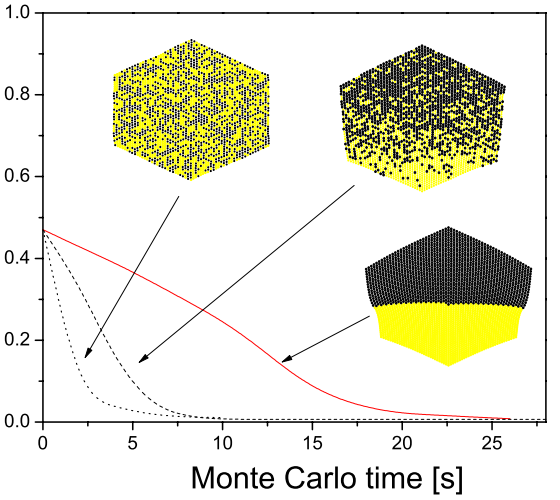

FIG. 9. (Color online) HS→LS relaxation curves after partial but perfectly homogeneous and nonhomogeneous photoexcitation. The latter is once shown with a gradient across the crystal and with a sharp frontier. All parameters are taken as the standard values given in the caption of Fig. 3.

homogeneous but incomplete photoexcitation can lead to an incorrect evaluation of the parameters governing the relaxation.

In Fig. 8 we present relaxation curves from different homogenous partial photoexcited states for a strongly cooperative system. Obviously, starting at a given HS fraction, with a completely random distribution of HS and LS molecules will result in a different relaxation curve than the one obtained for the same HS fraction, when starting after complete photoexcitation. The dotted lines in Fig. 8 correspond to relaxation curves displaced along the time axis. Whereas the curves starting at high HS fraction still present a sigmoidal shape, relaxation curves for $n_{HS}<0.5$ invariably start at a faster rate than observed for the full relaxation curve at the same HS fraction. As we have previously shown,[23] domains buildup during the relaxation and this will determine a nonrandom configuration as the relaxation proceeds. In fact, the initial slope for all relaxation curves must be identical to the slope obtained in the frame of a mean-field model. The results are similar as those provided by Monte Carlo simulations including both nearest-neighbors and long-range interactions and are in concordance with experimental data.[16]

Very often in practical applications the initial partial photoexcited state is not homogenous, for instance, because of a variation in the absorption cross section at different irradiation wavelengths or a gradient in irradiation intensity, or for polycrystalline samples because of a size distribution and problems associated with the penetration depth of the light. In the most common situation this results in gradients of the HS fraction within the sample, with a higher concentration in the front part of the sample. In Fig. 9, we illustrate the differences between the relaxation curves for the two extreme cases, that is for a partial but homogeneous population of the light-induced HS state and for a steplike distribution with one domain fully excited and the other one in the LS state, and for an exponentially decreasing light-induced HS fraction across the sample from front to rear. For all three curves the mean initial HS fraction is identical at $n_{HS}=0.48$. If the initial state has a steplike distribution, then the subsequent relaxation shape is still sigmoidal and close to that obtained from a complete photoexcited state except that it starts at a lower initial value. In contrast, the relaxation curve is much closer to single exponential when starting from a homogenous photoexcited state as already shown in Fig. 8. Although not single exponential, almost all the sigmoidal character is lost for a partial excitation with a realistic initial concentration gradient across the sample. Indeed, the results of the simulations on the basis of the simple model of mechanoelastic interaction solved exactly by the Monte Carlo procedure are confirmed by the experimental results obtained previously for the $[Fe_{0.5}Zn_{0.5}(btr)_2(NCS)_2]H_2O$ compound.[25]

IV. CONCLUSIONS

In this paper we have shown that the mechanoelastic model can be successfully applied to the characterization of various experimental phenomena observed in spin-crossover complexes under light irradiation. Especially the essential features of the phenomena of bistability and hysteresis behavior, important for their possible applications as full optical memories, are well reproduced with the simple model. A comparison with other models is presented and, in particular, it is shown that the present model is more powerful than mean-field models that cannot reproduce clusters, or than typical Ising-type models that usually need two *a priori* not known interaction parameters, instead of a single one as in the present approach. In the future we shall deal with a 3D model, able to reproduce the complex behavior of other important classes of spin-crossover complexes and for direct application to nanoparticles, which are currently being investigated experimentally by several research groups.[2–4,46]

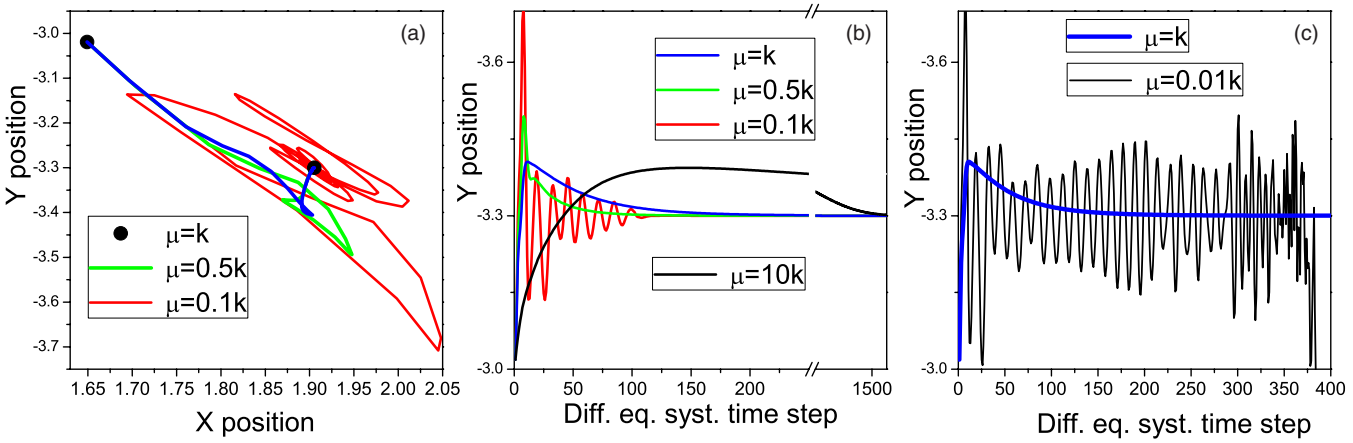

FIG. 10. (Color online) (a) Regardless of the spring constant value (if this value is not too small) the molecules arrive always at the same position after a Monte Carlo step but the path to mechanical equilibrium is different. (b) The time it takes for the equilibrium position to be established depends on the spring constant; if this constant is too big, more steps in solving the differential equations are necessary. (c) If the spring constant is too small, then the system enters into an uncontrolled oscillatory motion.

ACKNOWLEDGMENTS

This work was supported by Romanian CNCSIS-UEFISCSU, Project No. PNII RU-TE 185/2010 and by the Swiss National Science Foundation (Grant No. 200020-125175).The authors are indebted to Masamichi Nishino (National Institute for Materials Science—Tsukuba) and Seiji Miyashita (University of Tokyo) for helpful discussions.

APPENDIX

The choice of the damping constant is essential for the appropriate determination of the equilibrium positions of the molecules in the system. The final position of the molecules after solving the system of differential Eq. (3) is the same, regardless of the value of the damping constant. However, the way this final position is established depends on the damping constant: for small values of a given molecule effectuates an oscillatory motion with the amplitude quickly decreasing to zero (underdamped regime); for somewhat higher values the system converges to the equilibrium without oscillating, while for higher damping constants, the equilibrium is still obtained but after a very long time (overdamped regime).[47] This case is not favorable for simulations, as it will need more computing time. On the opposite, if the damping constant is too small, the system enters into an uncontrolled oscillatory motion that finally will destroy the hexagonal shape (Fig. 10).

*cristian.enachescu@uaic.ro

[1] I. Tudosa, C. Stamm, A. B. Kashuba, F. King, H. C. Siegmann, J. Stohr, G. Ju, B. Lu, and D. Weller, Nature (London) **428**, 831 (2004).

[2] I. Boldog, A. Gaspar, V. Martínez, P. Pardo-Ibanez, V. Ksenofontov, A. Bhattacharjee, P. Gutlich, and J. Real, Angew. Chem. **47**, 6433 (2008).

[3] E. Coronado, J. R. Galán-Mascarós, M. Monrabal-Capilla, J. García-Martínez, and P. Pardo-Ibánez, Adv. Mater. **19**, 1359 (2007).

[4] J. Larionova, L. Salmon, Y. Guari, A. Tokarev, K. Molvinger, G. Molnar, and A. Bousseksou, Angew. Chem. **120**, 8360 (2008).

[5] G. Molnár, S. Cobo, J. A. Real, F. Carcenac, E. Daran, C. Vieu, and A. Bousseksou, Adv. Mater. **19**, 2163 (2007).

[6] S. Cobo, G. Molnar, J. A. Real, and A. Bousseksou, Angew. Chem., Int. Ed. **45**, 5786 (2006).

[7] S. Bonhommeau, G. Molnar, A. Galet, A. Zwick, J. A. Real, J. J. McGarvey, and A. Bousseksou, Angew. Chem., Int. Ed. **44**, 4069 (2005).

[8] S. Cobo, D. Ostrovskii, S. Bonhommeau, L. Vendier, G. Molnar, L. Salmon, K. Tanaka, and A. Bousseksou, J. Am. Chem. Soc. **130**, 9019 (2008).

[9] S. Decurtins, P. Gutlich, C. P. Kohler, H. Spiering, and A. Hauser, Chem. Phys. Lett. **105**, 1 (1984).

[10] A. Hauser, Top. Curr. Chem. **234**, 155 (2004).

[11] A. Hauser, R. Hinek, H. Spiering, and P. Gutlich, Chem.-Eur. J. **2**, 1435 (1996).

[12] A. Desaix, O. Roubeau, J. Jeftic, J. G. Haasnoot, K. Boukheddaden, E. Codjovi, J. Linares, M. Nogues, and F. Varret, Eur. Phys. J. B **6**, 183 (1998).

[13] H. Spiering, T. Kohlhaas, H. Romstedt, A. Hauser, C. Bruns-Yilmas, J. Kusz, and P. Gutlich, Coord. Chem. Rev. **190-192**, 629 (1999).

[14] F. Varret, K. Boukheddaden, E. Codjovi, C. Enachescu, and J. Linares, Top. Curr. Chem. **234**, 199 (2004).

[15] H. Romstedt, A. Hauser, and H. Spiering, J. Phys. Chem. Solids **59**, 265 (1998).

[16] H. Romstedt, H. Spiering, and P. Gutlich, J. Phys. Chem. Solids **59**, 1353 (1998).

[17] K. Boukheddaden, J. Linares, H. Spiering, and F. Varret, Eur. Phys. J. B **15**, 317 (2000).

[18] O. Sakai, T. Ogawa, and K. Koshino, J. Phys. Soc. Jpn. **71**, 978

(2002).
[19] O. Sakai, M. Ishii, T. Ogawa, and K. Koshino, J. Phys. Soc. Jpn. **71**, 2052 (2002).
[20] M. Nishino, K. Boukheddaden, Y. Konishi, and S. Miyashita, Phys. Rev. Lett. **98**, 247203 (2007).
[21] Y. Konishi, H. Tokoro, M. Nishino, and S. Miyashita, Phys. Rev. Lett. **100**, 067206 (2008).
[22] L. Stoleriu, C. Enachescu, A. Stancu, and A. Hauser, IEEE Trans. Magn. **44**, 3052 (2008).
[23] C. Enachescu, L. Stoleriu, A. Stancu, and A. Hauser, Phys. Rev. Lett. **102**, 257204 (2009).
[24] E. Freysz, S. Montant, S. Letard, and J. F. Letard, Chem. Phys. Lett. **394**, 318 (2004).
[25] C. Enachescu, U. Oetliker, and A. Hauser, J. Phys. Chem. B **106**, 9540 (2002).
[26] M. Lorenc, J. Hebert, N. Moisan, E. Trzop, M. Servol, M. Buron-LeCointe, H. Cailleau, M. L. Boillot, E. Pontecorvo, M. Wulff, S. Koshihara, and E. Collet, Phys. Rev. Lett. **103**, 028301 (2009).
[27] S. Miyashita, P. A. Rikvold, T. Mori, Y. Konishi, M. Nishino, and H. Tokoro, Phys. Rev. B **80**, 064414 (2009).
[28] R. Bronisz, Inorg. Chem. **44**, 4463 (2005).
[29] I. Krivokapic, C. Enachescu, R. Bronisz, and A. Hauser, Chem. Phys. Lett. **455**, 192 (2008).
[30] A. B. Gaspar, V. Ksenofontov, J. A. Real, and P. Gutlich, Chem. Phys. Lett. **373**, 385 (2003).
[31] S. Miyashita, Y. Konishi, M. Nishino, H. Tokoro, and P. A. Rikvold, Phys. Rev. B **77**, 014105 (2008).
[32] W. Nicolazzi, S. Pillet, and C. Lecomte, Phys. Rev. B **78**, 174401 (2008).
[33] C. W. Gear, *Numerical Initial Value Problems in Ordinary Differential Equations* (Prentice-Hall, Englewood Cliffs, New Jersey, 1971).
[34] C. Enachescu, H. Constant-Machado, E. Codjovi, J. Linares, K. Boukheddaden, and F. Varret, Physica B **306**, 155 (2001).
[35] Y. Ogawa, S. Koshihara, K. Koshino, T. Ogawa, C. Urano, and H. Takagi, Phys. Rev. Lett. **84**, 3181 (2000).
[36] K. Koshino and T. Ogawa, J. Phys. Soc. Jpn. **68**, 2164 (1999).
[37] C. Enachescu, M. Nishino, S. Miyashita, A. Hauser, A. Stancu, and L. Stoleriu, EPL **91**, 27003 (2010).
[38] M. Nishino, C. Enachescu, S. Miyashita, K. Boukheddaden, and F. Varret, Phys. Rev. B **82**, 020409(R) (2010).
[39] K. Ichiyanagi, J. Hebert, L. Toupet, H. Cailleau, P. Guionneau, J. F. Letard, and E. Collet, Phys. Rev. B **73**, 060408 (2006).
[40] S. Pillet, V. Legrand, M. Souhassou, and C. Lecomte, Phys. Rev. B **74**, 140101 (2006).
[41] C. Chong, F. Varret, and K. Boukheddaden, Phys. Rev. B **81**, 014104 (2010).
[42] C. Chong, H. Mishra, K. Boukheddaden, S. Denise, G. Bouchez, E. Collet, J. C. Ameline, A. D. Naik, Y. Garcia, and F. Varret, J. Phys. Chem. B **114**, 1975 (2010).
[43] P. A. Rikvold, H. Tomita, S. Miyashita, and S. W. Sides, Phys. Rev. E **49**, 5080 (1994).
[44] C. Enachescu, R. Tanasa, A. Stancu, F. Varret, J. Linares, and E. Codjovi, Phys. Rev. B **72**, 054413 (2005).
[45] M. Nishino and S. Miyashita (private communication).
[46] F. Volatron, L. Catala, E. Riviere, A. Gloter, O. Stephan, and T. Mallah, Inorg. Chem. **47**, 6584 (2008).
[47] A. Papoulis, *Probability, Random Variables, and Stochastic Processes* (McGraw-Hill, New York, 1984).